Supporting Information

Clarifying the lithium storage behavior of MoS_2 with in situ electrochemical impedance spectroscopy

Chao Deng, Hongquan Wang, Shengping Wang*

Faculty of Materials Science and Chemistry, China University of Geosciences, Wuhan 430074, China

* Email: spwang@cug.edu.cn

$$MoS_2 + xLi^+ + xe^- \xrightarrow{\text{Discharge}} Li_xMoS_2 \quad \text{(S1)}$$

$$Li_xMoS_2 + (4-x)\,Li^+ + (4-x)e^- \xrightarrow{\text{Discharge}} 2Li_2S + Mo \quad \text{(S2)}$$

$$Li_2S + Mo - 2e^- \leftrightharpoons MoS_2 + 2Li^+ \quad \text{(S3)}$$

$$Li_2S - 2e^- \leftrightharpoons 2Li^+ + S \quad \text{(S4)}$$

During the discharging process, lithium ions are intercalated into the interlayer of MoS_2 to form Li_xMoS_2 (Formula S1). [1,2] Then, Li_xMoS_2 slowly transforms to metallic Mo and Li_2S when discharged to 0.01 V (*vs.* Li/Li^+) (Formula S2). [3,4] Some researchers believe that when recharged to 3.0 V (*vs.* Li/Li^+), Li_2S reacts with metallic Mo and continues to form MoS_2, which is the conversion between MoS_2 and metallic Mo in the later cycles (Formula S3). [5] Other researchers have believed that Li_2S is oxidized to elemental sulfur in the charging process, and metallic Mo no longer stores lithium as an active material. [6-9] Therefore, a conversion reaction occurs between sulfur and Li_2S, similar to the reaction mechanism of lithium-sulfur batteries (Formula S4). [10]

Program S1: Program of batch-fitting EIS data

```
from impedance import preprocessing
from impedance.models.circuits import CustomCircuit
from impedance.visualization import plot_nyquist
import numpy as np

def readtxt(filename):
    with open(filename, 'r') as input_file:
        lines = input_file.readlines()
    start_line = 1
    raw_data = lines[start_line:]
    f, Z = [], []
    for line in raw_data:
        each = line.split('\t')
        f.append(float(each[0]))
        Z.append(complex(float(each[1]), float(each[2])))
    input_file.close()
    return np.array(f), np.array(Z)
path="./ raw_data /" #Create a folder named ‘raw_data’ in the same level directory, and put the original data into this folder in the form of txt. document after grouping.
Fit_data=[]
for i in range(1,312):
    frequencies, Z = readtxt(path+str(i)+'.txt')
    frequencies, Z = preprocessing.ignoreBelowX(frequencies, Z)
    circuit = 'R0-p(R1,C1)-p(R2-Wo1,C2)' # Input equivalent circuit
    initial_guess = [.01, .01, 100, .01, .05, 100, 1]
    circuit = CustomCircuit(circuit, initial_guess=initial_guess)
    circuit.fit(frequencies, Z)
    print(' Serial number :%d '%i)
    print(circuit)
    Fit_data.append(circuit.parameters_)
Result = []
f=open('Test_Result.txt','w+')
for m in range(len(Fit_data)):
    jointsFrame = Fit_data[m]
    f.write('%d'%m)
    f.write(' ')
```

```
61          Result.append(jointsFrame)
62          for Ji in range(7):
63                  strNum =str(jointsFrame[Ji])
64                  f.write(strNum)
65                  f.write(' ')
66          f.write('\n')
67  f.close()
68
69
```

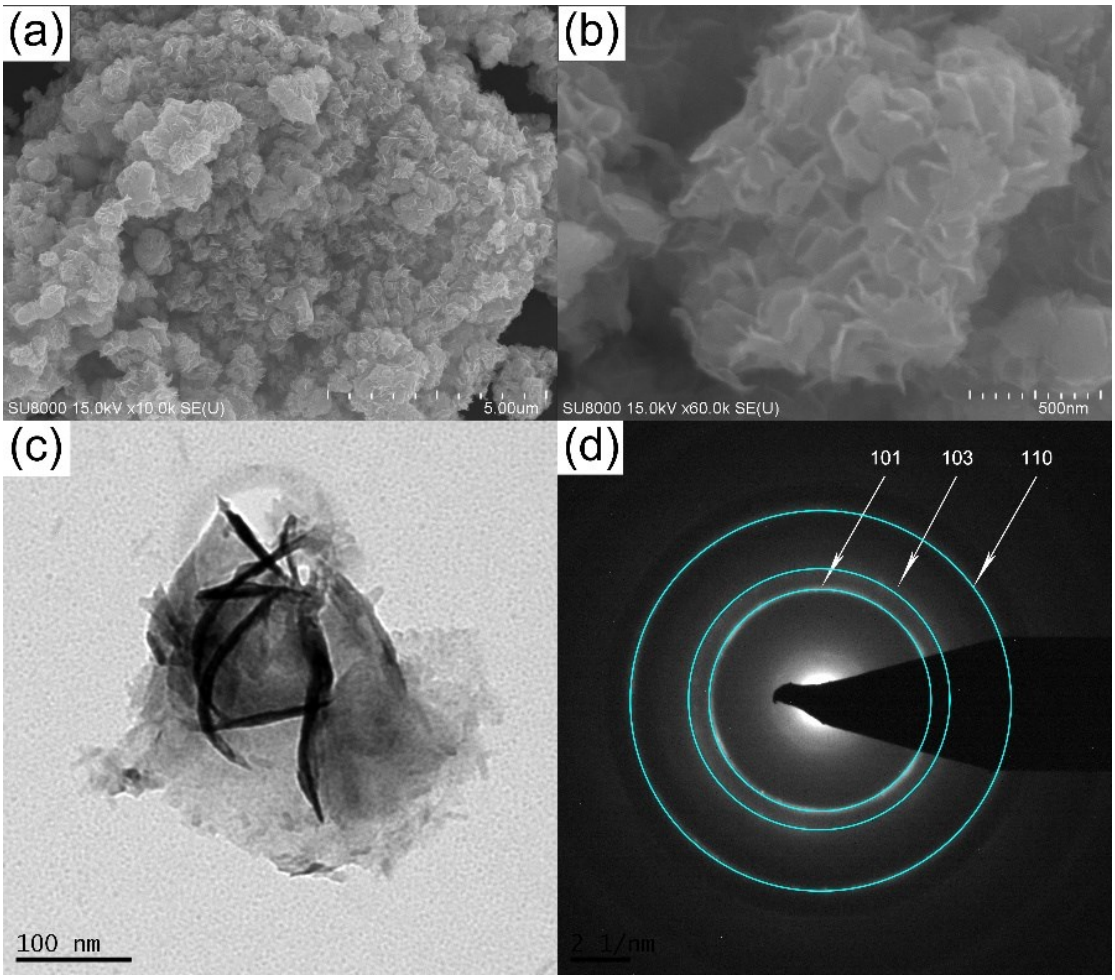

Fig. S1 SEM (a, b) and TEM images (c) and polycrystalline electron diffraction pattern (d) of the initial MoS_2.

The morphology of the initial MoS_2 prepared by the hydrothermal method is illustrated in Fig. S1. MoS_2 had a microsphere structure and aggregated into a block. The individual MoS_2 microspheres did not form a complete spherical structure, which was affected by the temperature and time of the hydrothermal reaction. [11] The single MoS_2 microspheres were composed of MoS_2 sheets, which promoted the migration of lithium ions (Fig. S1b). [12] In addition, the structure also increased the contact area of MoS_2 and the electrolyte, thereby increasing the utilization of active materials. [13] The nanosheet structure of MoS_2 was further demonstrated by TEM. As shown in Fig. S1c, the MoS_2 nanosheets had a lamellar structure. The corresponding selected area electron diffraction (SAED) pattern also confirmed the formation of MoS_2 (Fig. S1d). The three diffraction rings of the SAED pattern could be indexed to the (101), (103), and (110) planes of MoS_2. [14]

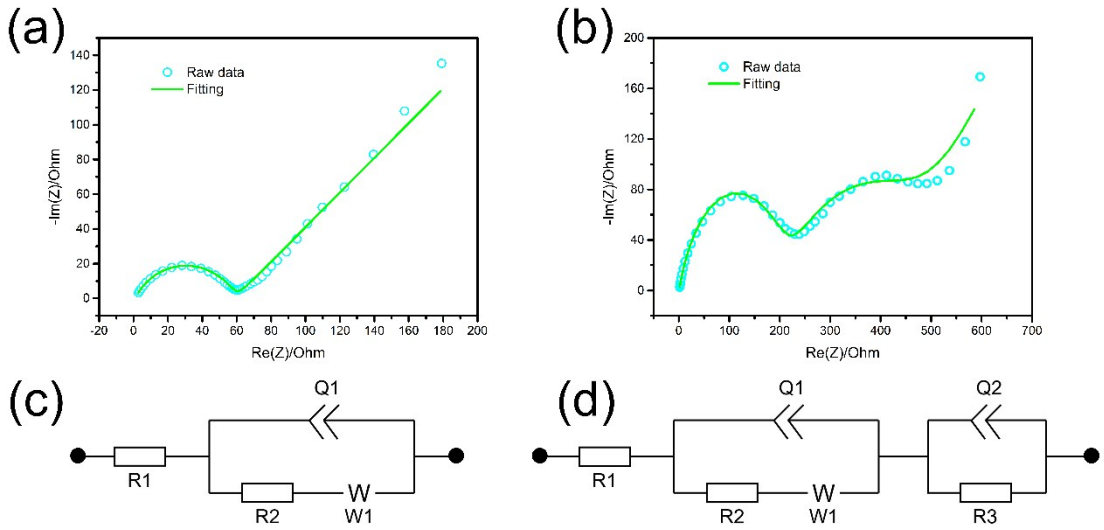

Fig. S2 EIS spectra and the corresponding equivalent circuits of MoS_2 at 2.27 V (a, c) and 0.76 V (b, d) in the first charging process at 0.1 mA cm^{-2} from 3.0 V to 0.01 V.

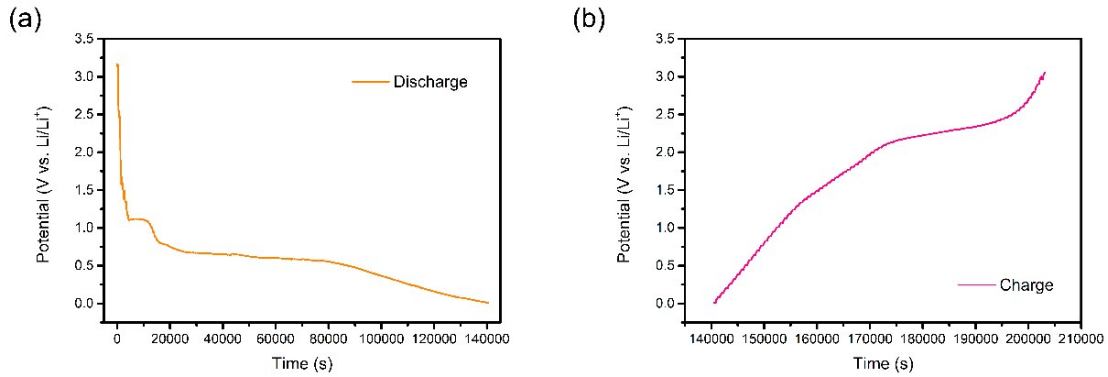

Fig. S3 First discharge (a) and charge (b) curves of MoS_2 at 0.1 mA cm^{-2} from 3.0-0.01 V with a step-by-step EIS test.

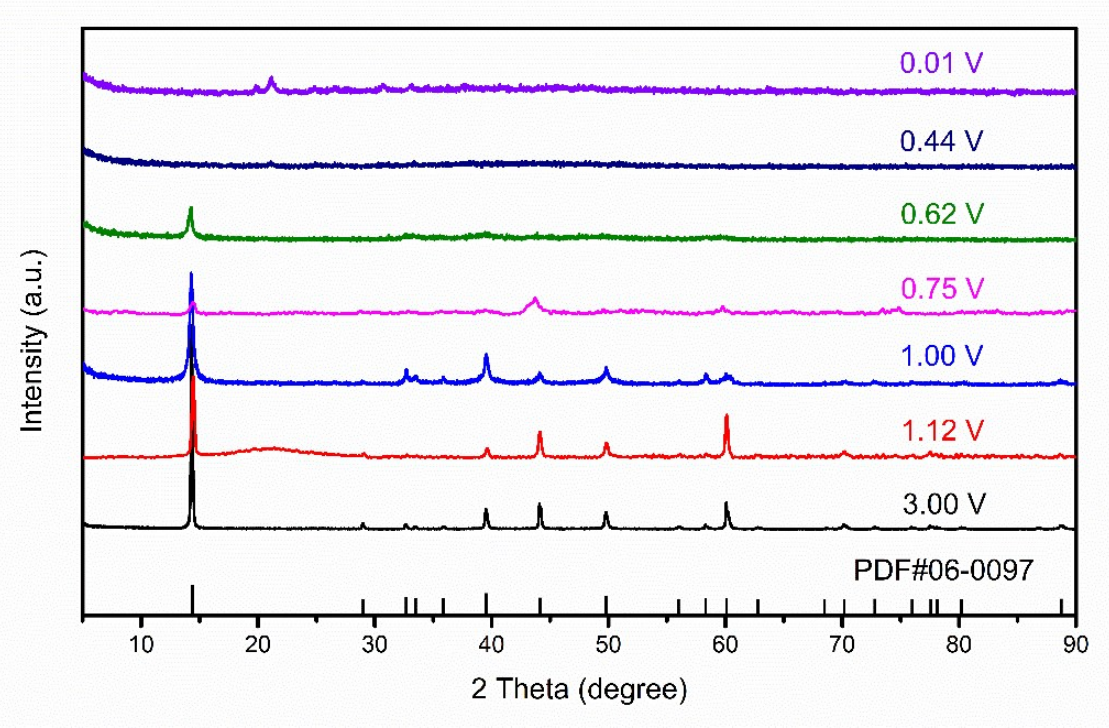

Fig. S4 XRD patterns of MoS_2 in the first discharging process at 0.1 mA cm^{-2}.

To determine the reactions that occurred in each potential range, the product of each reaction stage needed to be characterized. Based on the phases identified by EIS, the battery was decomposed, and XRD was performed at the end of each stage. The result is shown in Fig. S4.

Stage a: 3.0-1.12 V

Before the EIS test, the MoS_2 electrode was tested by XRD, and the results are shown in Fig. S4. The initial potential of the MoS_2 electrode without discharging was approximately 3.0 V. Comparing the experimental data with the standard card, the diffraction peak of MoS_2 agreed well with the standard card (PDF#06-0097), indicating that MoS_2 was successfully synthesized by the hydrothermal method. [4] The diffraction peaks at 14.5°, 29°, 39°, and 45° correspond to the (002), (004), (103) and (106) planes of MoS_2, respectively. [15]

According to the standard card, the structure of MoS_2 did not change when discharging to 1.12 V, demonstrating that the structure of MoS_2 was preserved. Additionally, note that the peak at 14.49° corresponding to the (002) plane of MoS_2 did not move, indicating that the layer spacing of MoS_2 did not change.

Stage b: 1.12-1.0 V

As shown in Fig. 2g, there was an obvious platform that appeared in this potential range, and in the differential capacitance curve, it corresponded to peak 1. Comparing the XRD pattern of the 1.0 V and 1.12 V samples shown in Fig. S4, the XRD pattern did not change greatly, indicating that the

layered structure of MoS_2 had not been damaged. Then, the diffraction peak corresponding to the (002) plane shifted to the left (Fig. S5), suggesting that the interlayer distance of MoS_2 increased. The reason for this phenomenon was that lithium ions were intercalated between the layers of MoS_2. [16,17] In addition, as shown in Fig. 1a, when the charge and discharge window was 1.0-3.0 V, MoS_2 had better cycle stability, indicating that the intercalation and extraction of lithium ions at this stage did not cause the structure of MoS_2 to be destroyed. Therefore, the intercalation and extraction of lithium ions in this potential range were reversible.

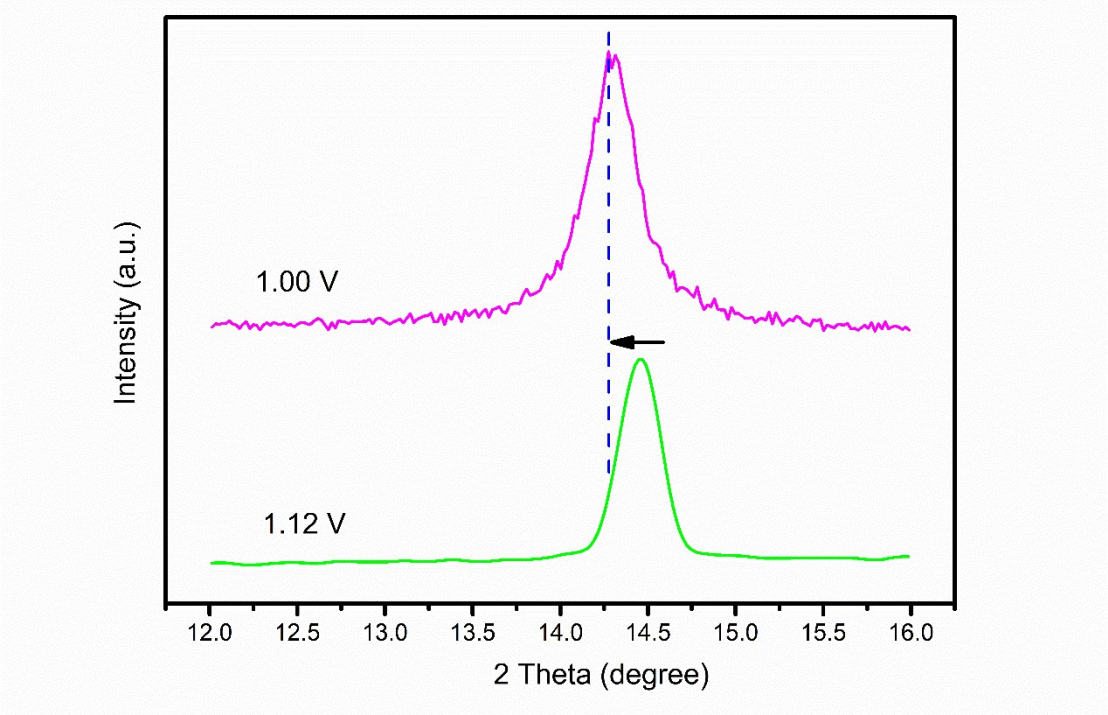

Fig. S5 Enlarged view of Fig. S4.

Stage c: 1.0-0.75 V

In a previous study, [18] this potential range was always ignored, but it was analyzed by a differential capacitance curve in this work (Fig. 2g). By analyzing the XRD patterns, the characteristic peaks of MoS_2 did not completely disappear within this potential range. The characteristic peaks at 14°, 44°, and 60° were still present, but the peak strengths decreased, indicating that the structure of MoS_2 changed greatly, but MoS_2 did not completely disappear at this stage. This may be because the number of MoS_2 particles decreases as lithiation progresses. [6]

Stage d: 0.75-0.62 V

As shown in Fig. S4, the diffraction peaks at 44° and 60° completely disappeared in the XRD pattern from 0.75 V to 0.62 V, but diffraction peaks at 14° were still present, demonstrating that some MoS_2 had been converted, although some was still present. The electrochemical reaction in stage d was a conversion reaction. Li^+ continued to enter Li_xMoS_2, and Li_xMoS_2 gradually converted

into elemental Mo and Li_2S. [19]

Stage e: 0.62-0.44 V

Fig. S4 shows that no diffraction peak was detected in the XRD pattern at the end of this period, suggesting that MoS_2 was completely converted into elemental Mo and Li_2S. [20] In terms of MoS_2, when the minimum potential of the charge/discharge window was lower than 0.6 V, the cycle stability of MoS_2 was reduced, indicating that the structure of MoS_2 was destroyed within this range.

Stage f: 0.44-0.01 V

When discharging to 0.01 V, a new diffraction peak appeared in the XRD pattern, which demonstrated that a new material had been produced at this stage. As shown in Fig. S6, the material corresponding to this Li_2MoO_4 diffraction peak (PDF#12-0762) suggests that Mo metal, lithium salt, and the electrolyte would react and form Li_2MoO_4 in the last stage of the reaction. [21] However, comparing the diffraction peaks of Li_2MoO_4 and MoS_2 shows that the intensities of the Li_2MoO_4 peaks are weak, which means that the content of Li_2MoO_4 is low.

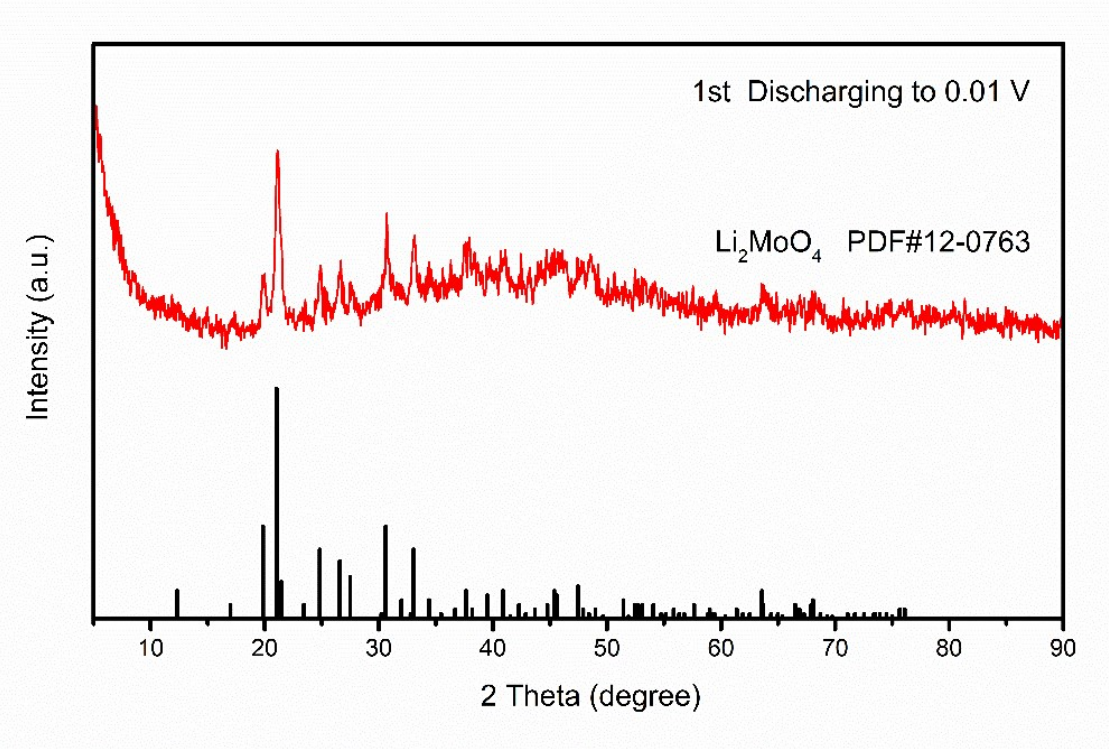

Fig. S6 XRD pattern of MoS_2 discharged to 0.01 V at 0.1 mA cm^{-2}.

Stage g: 0.01-1.20 V

As depicted in Fig. S7, the electrode was composed of Li_2MoO_4 and Li_2S at the end of the discharging process. The characteristic peaks of Li_2MoO_4 did not disappear when charging to 1.2 V, indicating that Li_2MoO_4 did not decompose at this stage. It could also be deduced from the

differential capacitance that there were no obvious characteristic peaks at this stage (Fig. S7). However, this stage could provide a charging capacity of approximately 230 mAh g^{-1}. Additionally, this potential did not reach the oxidation potential of Li_2S. This capacitance and potential had a linear relationship, which was very similar to the characteristics of the capacitor. [22]

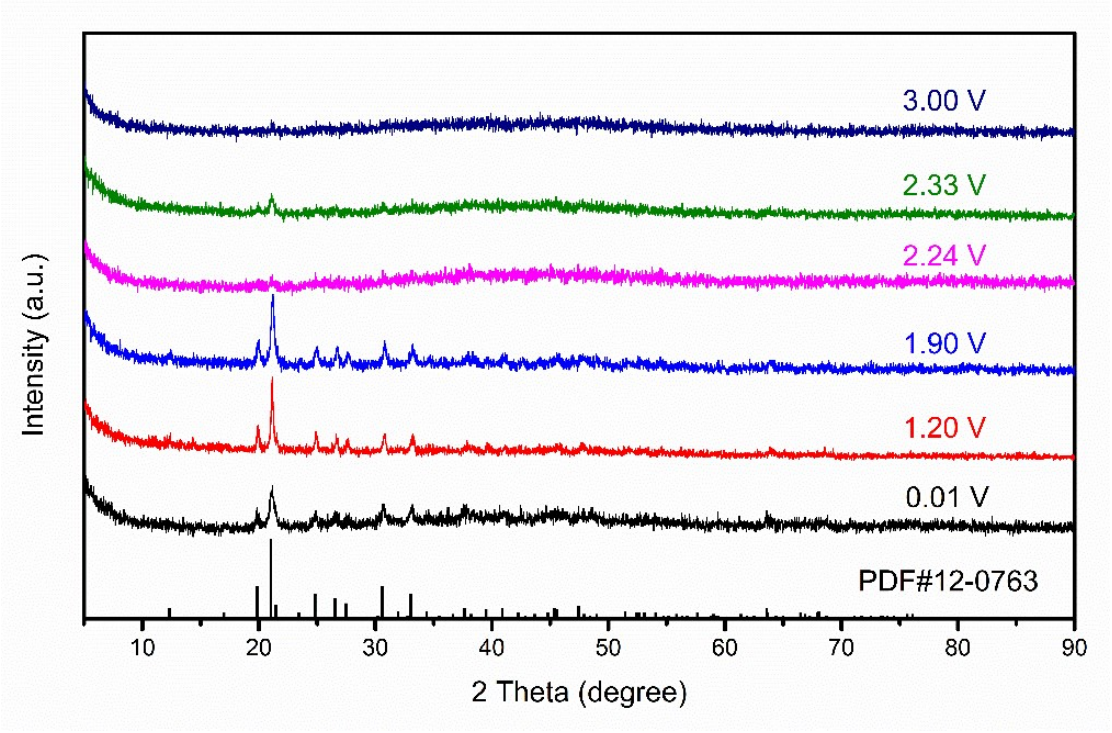

Fig. S7 XRD patterns of MoS_2 in the first charging process at 0.1 mA cm^{-2}.

Stage h: 1.20-1.90 V

When charging to 1.9 V, the characteristic peaks of Li_2MoO_4 were still present (Fig. S7), demonstrating that Li_2MoO_4 was not converted into other substances.

Stage i: 1.90-2.24 V

When charging to 2.24 V, the characteristic peaks of Li_2MoO_4 disappeared completely, indicating that the reaction in this stage was the conversion reaction of Li_2MoO_4. In the differential capacitance curve shown in Fig. 3f, a strong oxidation peak could also be observed, which meant that the reaction was a phase change reaction. However, the XRD pattern did not indicate the identity of the Li_2MoO_4 delithiation product, which may be due to the product being an amorphous substance.

Stage j: 2.24-2.33 V

When the potential of the electrode increased from 2.24 V to 2.33 V, no new diffraction peak appeared in the XRD pattern (Fig. S7), suggesting that no crystals of large particles were generated.

Stage k: 2.33-3.00 V

In the last stage of charging, no characteristic peak of MoS_2 was found in the XRD patterns, indicating that MoS_2 did not form after the first deep discharging process, which indicated once again that the reaction in the first cycle was an electrochemically irreversible process.

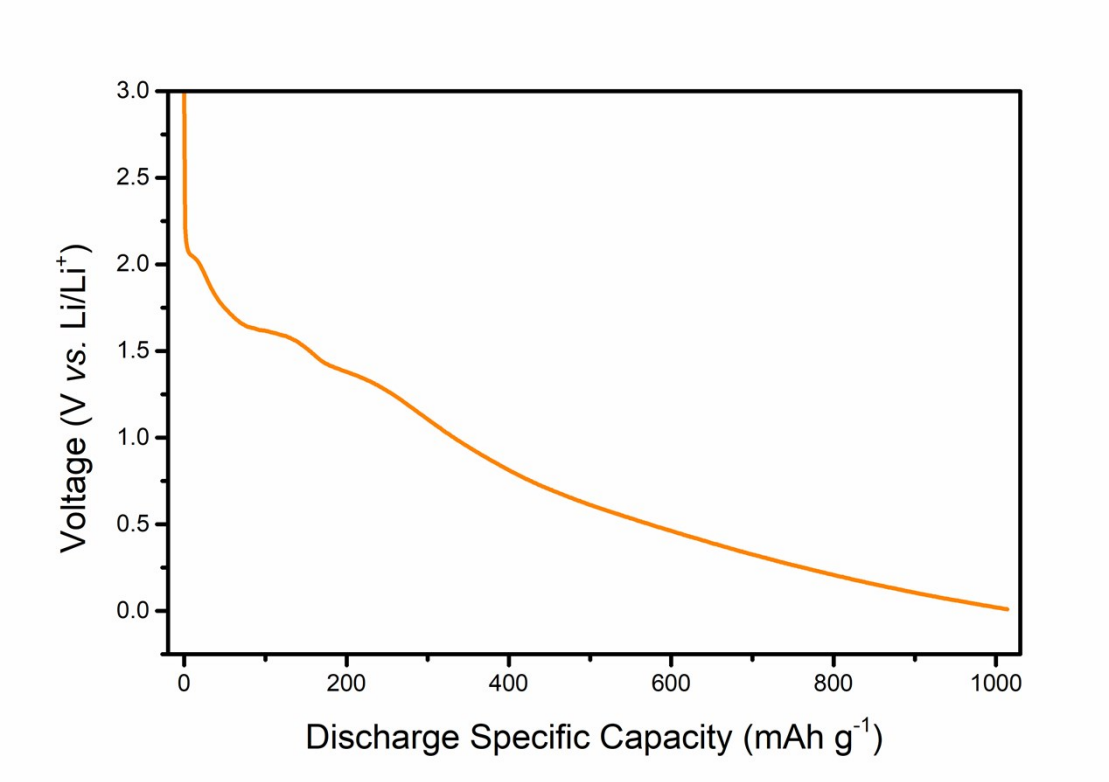

Fig. S8 Second galvanostatic discharge curve of MoS_2 at 0.1 mA cm^{-2} from 3.0 V to 0.01 V.

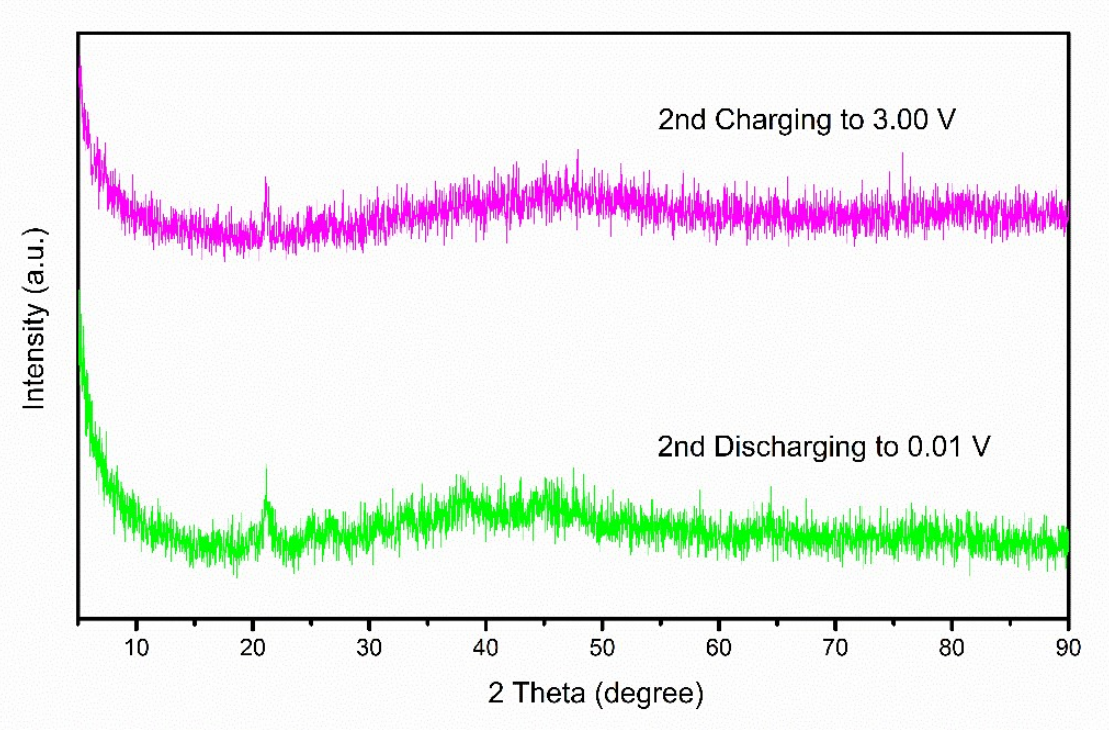

Fig. S9 XRD patterns of MoS_2 discharged to 0.01 V for the second time and charged to 3.0 V for the second time at 0.1 mA cm^{-2}.

209

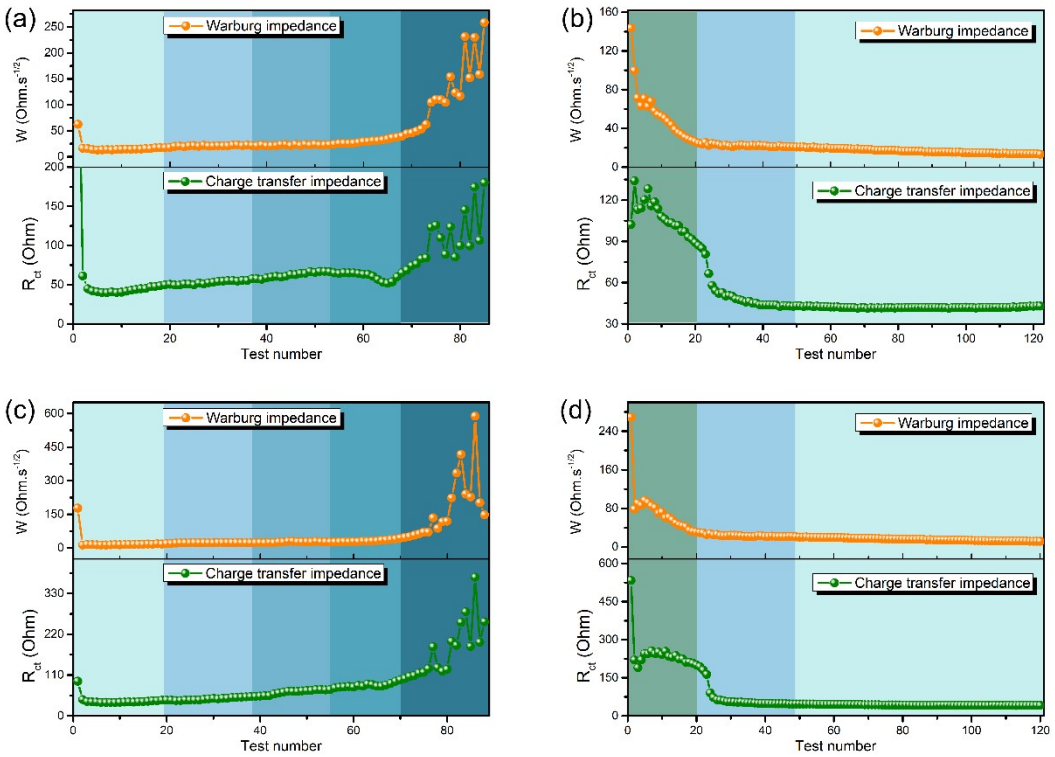

210

211 **Fig. S10** Impedances in the second (a) and third (c) charging processes and the third (b) and fourth

212 (d) discharging processes at 0.1 mA cm^{-2}.

213

214

References

[1] N. Imanishi, M. Toyoda, Y. Takeda, O. Yamamoto, Study on lithium intercalation into MoS_2, *Solid State Ionics*, 1992, 58, 333-338. https://doi.org/10.1016/0167-2738(92)90137-E

[2] L. Wang, Z. Xu, W. Wang, X. Bai, Atomic mechanism of dynamic electrochemical lithiation processes of MoS_2 nanosheets, *J. Am. Chem. Soc.*, 2014, 136, 6693-6697. https://doi.org/10.1021/ja501686w

[3] T. Stephenson, Z. Li, B. Olsen, D. Mitlin, Lithium ion battery applications of molybdenum disulfide (MoS_2) nanocomposites, *Energy Environ. Sci.*, 2014, 7, 209-231. https://doi.org/10.1039/c3ee42591f

[4] J. Gao, J. He, N. Wang, X. Li, Z. Yang, K. Wang, Y. Chen, Y. Zhang, C. Huang, Robust C-S bond integrated graphdiyne-MoS_2 nanohybrids for enhanced lithium storage capability, *Chem. Eng. J.*, 2019, 373, 660-667. https://doi.org/10.1016/j.cej.2019.05.086

[5] Q. Su, S. Wang, M. Feng, G. Du, B. Xu, Direct studies on the lithium-storage mechanism of molybdenum disulfide, *Sci. Rep.*, 2017, 7, 7275. https://doi.org/10.1038/s41598-017-07648-0

[6] Z. Zeng, X. Zhang, K. Bustillo, K. Niu, C. Gammer, J. Xu, H. Zheng, In situ study of lithiation and delithiation of MoS_2 nanosheets using electrochemical liquid cell transmission electron microscopy, *Nano Lett.*, 2015, 15, 5214-5220. https://doi.org/10.1021/acs.nanolett.5b02483

[7] L. Zhang, D. Sun, J. Kang, J. Feng, H.A. Bechtel, L.-W. Wang, E.J. Cairns, J. Guo, Electrochemical reaction mechanism of the MoS_2 electrode in a lithium-ion cell revealed by in situ and operando X-ray absorption spectroscopy, *Nano Lett.*, 2018, 18, 1466-1475. https://doi.org/10.1021/acs.nanolett.7b05246

[8] X. Fang, X. Guo, Y. Mao, C. Hua, L. Shen, Y. Hu, Z. Wang, F. Wu, L. Chen, Mechanism of lithium storage in MoS_2 and the feasibility of using Li_2S/Mo nanocomposites as cathode materials for lithium-sulfur batteries, *Chem. Asian J.*, 2012, 7, 1013-1017. https://doi.org/10.1002/asia.201100796

[9] M. Wu, C. Liu, T. Ma, M. Tang, J. Shen, H. Ji, G. Yang, Heterostructural composite of few-layered MoS_2/hexagonal MoO_2 particles/graphene as anode material for highly reversible lithium/sodium storage, *Int. J. Energy Res.*, 2020, 44, 518-527. https://doi.org/10.1002/er.4963

[10] X. Hong, R. Wang, Y. Liu, J. Fu, J. Liang, S. Dou, Recent advances in chemical adsorption and catalytic conversion materials for Li-S batteries, *J. Energy Chem.*, 2020, 42, 144-168. https://doi.org/10.1016/j.jechem.2019.07.001

[11] Q. Wang, J. Li, Facilitated lithium storage in MoS_2 overlayers supported on coaxial carbon nanotubes, *J. Phys. Chem. C*, 2007, 111, 1675-1682. https://doi.org/10.1021/jp066655p

[12] A. Enyashin, S. Gemming, G. Seifert, Nanosized allotropes of molybdenum disulfide, *Eur. Phys. J. Special Topics*, 2007, 149, 103-125. https://doi.org/10.1140/epjst/e2007-00246-0

[13] X. Qian, G. Zhu, K. Wang, F. Zhang, K. Liang, W. Luo, J. Yang, Bowl-like mesoporous polymer-induced interface growth of molybdenum disulfide for stable lithium storage, *Chem. Eng. J.*, 2020, 381, 122651. https://doi.org/10.1016/j.cej.2019.122651

[14] K. Chang, W. Chen, L-cysteine-assisted synthesis of layered MoS_2/graphene composites with excellent electrochemical performances for lithium ion batteries, *ACS Nano*, 2011, 5, 4720-4728. https://doi.org/10.1021/nn200659w

[15] Z. Wang, T. Chen, W. Chen, K. Chang, L. Ma, G. Huang, D. Chen, J.Y. Lee, CTAB-assisted synthesis of single-layer MoS_2-graphene composites as anode materials of Li-ion batteries, *J. Mater. Chem. A*, 2013, 1, 2202-2210. https://doi.org/10.1039/c2ta00598k

[16] J. Xu, Y. Xu, G. Tang, H. Tang, H. Jiang, The novel g-C_3N_4/MoS_2/ZnS ternary nanocomposite with enhanced lithium storage properties, *Appl. Surf. Sci.*, 2019, 492, 37-44. https://doi.org/10.1016/j.apsusc.2019.05.139

[17] J. Zong, F. Wang, G. Liu, M. Zhao, S. Yang, X. Song, Ethylene glycol solvent induced expansion of interplanar spacing and 2H-1T phase transformation of molybdenum disulfide nanocomposites for enhanced lithium storage capability, *J. Alloy. Compd.*, 2019, 810, 151959. https://doi.org/10.1016/j.jallcom.2019.151959

[18] H. Xue, Q. Jiao, J. Du, S. Wang, C. Feng, Q. Wu, H. Li, Q. Lu, D. Shi, Y. Zhao, Hollow MoS_2/rGO composites as high-performance anode materials for lithium-ion batteries, *Ionics*, 2019, 25, 4659-4666. https://doi.org/10.1007/s11581-019-03041-1

[19] T. Hwang, J. Lee, J. Oh, J.M. Kim, Y. Jeon, S.-K. Park, Y. Piao, Facile synthesis of crumpled nitrogen-doped carbon/molybdenum disulfide hybrid sheets as high-rate anodes for lithium-ion batteries, *Electrochim. Acta*, 2019, 319, 596-605. https://doi.org/10.1016/j.electacta.2019.07.018

[20] S. Hu, W. Chen, J. Zhou, F. Yin, E. Uchaker, Q. Zhang, G. Cao, Preparation of carbon coated MoS_2 flower-like nanostructure with self-assembled nanosheets as high-performance lithium-ion battery anodes, *J. Mater. Chem. A*, 2014, 2, 7862-7872. https://doi.org/10.1039/c4ta01247j

[21] L. Wang, Q. Zhang, J. Zhu, X. Duan, Z. Xu, Y. Liu, H. Yang, B. Lu, Nature of extra capacity in MoS_2 electrodes: molybdenum atoms accommodate with lithium, *Energy Storage Mater.*, 2019, 16, 37-45. https://doi.org/10.1016/j.ensm.2018.04.025

[22] Z. Du, S. Zhang, Y. Xing, X. Wu, Nanocone-arrays supported tin-based anode materials for lithium-ion battery, *J. Power Sources*, 2011, 196, 9780-9785. https://doi.org/10.1016/j.jpowsour.2011.08.012